VOL. 17, NO. 23, DECEMBER 2022 ISSN 1819-6608
ARPN Journal of Engineering and Applied Sciences

www.arpnjournals.com

DIELECTRIC PROPERTIES OF RAW ASTER TATARICUS AND ITS RESIDUE OF DECOCTION

Ong H. L.[1], Cheng E. M.[1,2], Mohamad C. W. S. R.[1], Beh C. Y.[1] and Khor S. F.[3]
[1]Faculty of Electronic Engineering Technology, University Malaysia Perlis (UniMAP), Pauh Putra Campus, Arau, Perlis, Malaysia
[2]Advanced Communication Engineering (ACE) Centre of Excellence, Universiti Malaysia Perlis, Jalan Tiga, Pengkalan Jaya Business Centre, Kangar, Perlis, Malaysia
[3]Centre of Excellence for Renewable Energy (CERE), Faculty of Electrical Engineering Technology (FTKE), Universiti Malaysia Perlis, Pauh Putra Campus, Arau, Perlis, Malaysia
E-Mail: emcheng@unimap.edu.my

ABSTRACT

The plant *Aster tataricus* is widely used in traditional Chinese medicine to relieve cough-related illnesses. In this work, the dielectric properties of *Aster tataricus* were studied in terms of dielectric constant (ε'), dielectric loss factor (ε"), and electrical conductivity (σ). A Hioki IM3570 impedance analyser and an Agilent E5071C ENA series vector network analyser were used for the impedance and dielectric measurement, respectively. The dielectric properties were investigated from 12.5 kHz to 5 MHz and 50 MHz to 20GHz. All the measurements were conducted at room temperature. *Aster tataricus* were dried and ground into powder for preparation of pellets before and after decoction. It can be noticed that the variation of measured dielectric constant, dielectric loss factor, and electrical conductivity are significant over frequency.

Keywords: aster tataricus, dielectric constant, loss factor, electrical conductivity.

INTRODUCTION

The flowering plant *Aster tataricus* (AT), akaZiwan. It is derived from the dried roots and rhizomes of *Aster tataricus* L. f. (Compositae) [1]. AT is a perennial plant that is found in East Asian countries, e.g., mainland China, South Korea, and Japan [2]. AT is one of the most commonly used traditional Chinese herbs recorded in Chinese pharmacopoeia[3]. Its roots and rhizomes have been used as a herbal material to assist in the treatments of cough, moisturization of the lungs, and elimination of phlegm [4], [5]. Several bioactive compounds in AT have been identified by previous studies, such as shion one, epifriedelinol, quercetin, emodin, caffeoylquinic acid, kaempferol, and some other triterpenes or saponins [6].

The decoction method is a usual method that is implemented by herb consumers, especially in Chinese communities. Decoction method is simple and user-friendly and it does not require any sophisticated tools. This method can be conducted domestically since this method uses only water as a solvent. However, the efficiency of this method in extracting the required bioactive compound (phytochemical contents) is not consistent. The required bioactive compound might yet be extracted in decoction, but it remains in the residues of herbs. Hence, it is required to develop a sensing system for decoction and residues of herbs to gauge the quality of decoction. In this work, a dielectric spectroscopic technique is implemented to characterize the decoction and its residues.

Dielectric properties of a material depict the dielectric behaviour of a material on exposure to a dynamic electric field [7], [8]. The electric and magnetic forces generated by the electromagnetic fields interact with materials in two ways: energy storage and energy dissipation[9]. Energy storage describes the lossless portion of the exchange of energy between the electromagnetic field and the material. The dielectric constant depicts the capability of a material to accumulate electrical energy due to the presence of an electric field. Energy dissipation occurs when electromagnetic energy is absorbed or dissipated in the material. The dielectric loss factor is the dissipation of electrical energy in the form of losses. The dielectric properties of the material are a direct consequence of its structure, content, and composition[10]. The function of dielectric constant and loss factor are frequency, temperature, and chemical parameters of organic composition [7], [11]. The frequency dependence translates into relaxations and resonances of the complex permittivity. It can be associated with various polarisation phenomena[8], [12], [13].

Dielectric spectroscopy measurement is widely used to characterise and identify dielectric behaviours of material. The characterization process relies on extracting the dielectric and conductive properties of the material under test from reflected and transmitted microwave signals [8]. It offers the advantage of being non-destructive, label-free, and covers a wide band of frequencies [14]. Dielectric properties of herbal plants could reflect the presented moisture content characteristics of chemical substances [7], [15]. Dielectric properties of plants exhibit frequency dependence. These properties are intrinsic properties of the constituent substances[15].In past studies, dielectric properties were used to determine the quality of fruits [16], agricultural products [17], and foods [18]. The relation between frequency and dielectric properties is useful in determining the optimum frequency range in which the AT has the desired dielectric characteristics for intended applications [19].

METHODOLOGY

Sample Preparation

Aster tataricus (AT) is commercially available. The herb was dried for 24 hours at 40°C. It was ground to

be fine powder and sealed in a vessel. Ground AT was soaked in distilled water eight times for 30 min and boiled at 85 °C for 2 hours [20]. The residue was collected and further dried for 24 hours at 40°C. Likewise, the residue was ground to be fine powder and it was sealed in the vessel too before dielectric measurement. The raw AT in powder and decocted AT were prepared in cylindrical pellets (20 mm in diameter) using a hydraulic press.

Sample Measurements

An impedance analyser (IM3570, HIOKI) with an L2000 4-terminal probe was used to conduct the impedance measurements (parallel capacitance and conductance). The parallel capacitance (C_p) and conductance (G) of the cylindrical pellets were measured from 12.5 kHz to 5 MHz with an oscillated voltage of 1.0 V. This measurement was conducted at room temperature (25 °C). ε′ and ε″ are the real part and imaginary part of the complex dielectric permittivity (ε∗), respectively, as expressed in Equation (1):

$$\varepsilon^* = \varepsilon' - j\varepsilon'' \quad (1)$$

where $j = \sqrt{-1}$. ε′, ε″ andσ of material under test are functions of the C_p and G, as written in Equation (2), Equation (3), and Equation (4):

$$\varepsilon' = \frac{C_p d}{A\varepsilon_0} \quad (2)$$

$$\varepsilon'' = \frac{Gd}{\omega A\varepsilon_0} \quad (3)$$

$$\sigma = \frac{Gd}{A} \quad (4)$$

where A is the sample area, d is the sample thickness, ε_o is the free space permittivity (8.85×10^{-12}F/m), and ω=2πf is the angular frequency[21], [22].

The dielectric measurement was conducted by using Agilent Technologies open-ended coaxial-line probe in conjunction with an Agilent Technologies E5071C ENA series vector network analyser. The network analyser and the probe need to be calibrated. Air, water, and shorting block were used as the calibration standards to ensure consistency and accuracy of measurements without disturbance of systematic errors. ε′ and ε″ of the sample were measured with Agilent Technologies 85070E dielectric probe kit software from 50 MHz to 20 GHz at room temperature (25 °C).

RESULTS AND DISCUSSIONS

Dielectric Measurement

Impedance analyser (IM3570, HIOKI)

ε′ and ε″ of raw AT pellets and decocted AT pellets were measured at 12.5 kHz to 5 MHz frequency range. The variation of ε′ and ε″ over log frequency (Hz) from 12.5 kHz to 5 MHz are shown in Figure-1 and Figure-2, respectively. All the measurements were conducted at room temperature (25 °C). It is observed that the ε′ and ε″ of raw AT pellets are decocted AT pellets is high at low frequencies and decrease when frequency increases. Raw AT pellets have higher ε′ and ε″ than decocted AT pellets. The orientation and interfacial polarizations lead to the variation of ε′ and ε″. The orientation polarization occurs when the permanent dipole molecules are subjected to the time-varying electric field. The interfacial polarization takes place due to the material phases with different dielectric permittivity and electrical conductivity[22]. It can be observed that ε′ and ε″ are nonlinear with respect to the frequency at a constant temperature. This decrease is mild at high frequencies for both AT pellets as shown in Figure-1 and Figure-2. This might be mainly ascribed to the space charges of the samples having insufficient time to realign with the oscillation of the applied electric field [23]. It implies that the polarization mechanism is switched from low to high frequency.

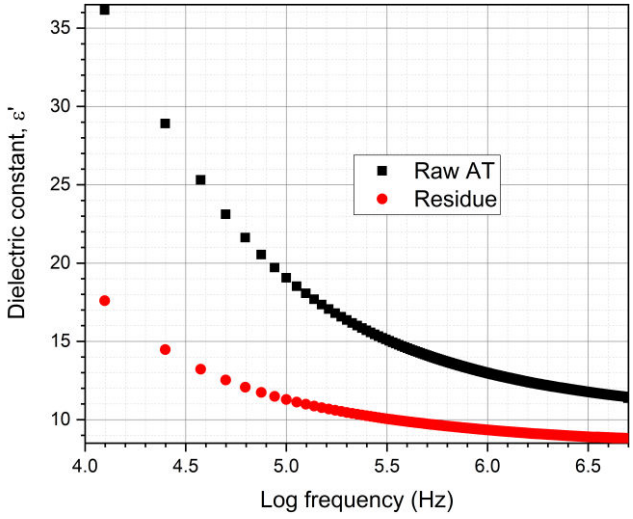

Figure-1. Dielectric constant, ε′ with log frequency (Hz).

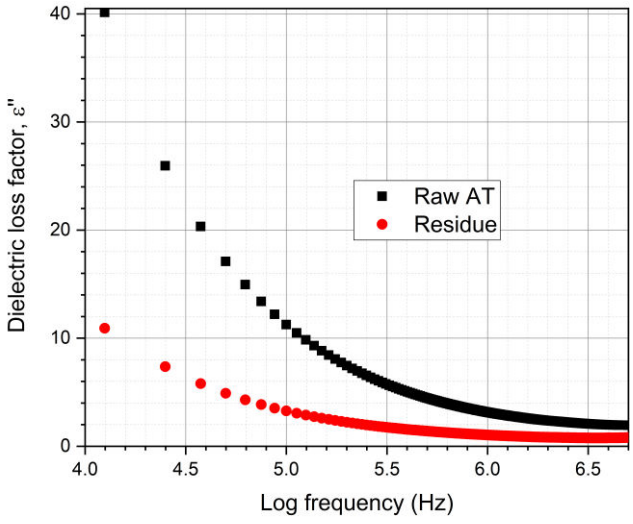

Figure-2. Dielectric loss factor, ε″ with log frequency (Hz).

Figure-3 shows the variation of electrical conductivity over log frequency (Hz), from 12.5 kHz to 5 MHz at room temperature. The electrical conductivity of raw AT is higher than residue. It might be due to the higher element content found in raw AT than in residue [24]. This is attributed to the extraction efficiency of elements during decoctions [25]. In the previous study, metallic elements in AT decoction, e.g., Mg, Mn, Cu, Zn, Se, and Mo were determined by using the ICP-MS technique [26]. These elements' content from the raw AT diffuses into the extract during decoction. Hence, it makes sense that the residue shows lower electrical conductivity than raw AT. Besides, the electrical conductivity of raw AT and residue increases when frequency increases. At low frequencies, the applied electric field forces the charge carriers to drift over large distances. When the frequency increases, the mean displacement of the charge carriers is reduced. As a result, it shows that the electrical conductivity of raw AT and residue follows the law of hopping conduction [27]. The hopping process refers to the abrupt movement of a charge carrier from one location to another (charge migration). In other words, small mean displacement facilitates the charge migration that led to electric conduction.

On the other hand, the synchrony between oscillated charge and applied field plays a vital role in determining conductivity. High synchrony between the applied field and oscillated charge along the functional groups of polyphenols during polarization at high frequency led to low ε″. This response implies that the charge oscillation is resistanceless in the media. In other words, the media has high conductivity when the frequency is high.

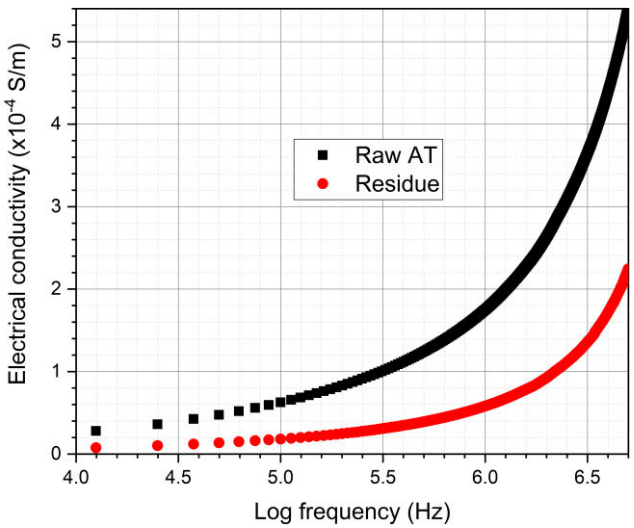

Figure-3. Electrical conductivity (x10^{-4} S/m) with log frequency (Hz).

Agilent E5071C ENA series vector network analyser

ε′ and ε″ of raw AT and residue were measured at 50 MHz to 20GHz frequency range. The variation of ε′ and ε″ with frequency (Hz), from 50 MHz to 20GHz are shown in Figure-4 and Figure-5, respectively. All the measurements were conducted at room temperature (25 °C). It can be observed that ε′ of raw AT and residue are high at low frequencies. It decreases when frequency increases as shown in Figure-4. This decrement is insignificant at high frequencies for both raw AT and residue. On the other hand, ε″ is low at low frequencies. It increases with frequency as shown in Figure-5. Raw AT has higher ε′ and ε″ than residue. The variation of ε′ and ε″ is due to the orientation and interfacial polarizations. When permanent dipole molecules are exposed to a time-varying electric field, orientation polarisation occurs. However, interfacial polarisation takes place because the material phases with different dielectric permittivity and electrical conductivity [22]. At constant temperature, ε′ and ε″ are shown to be nonlinear with respect to frequency. This decrement with a low gradient can be noticed at high frequencies for both raw AT and residue. This might be ascribed to the dipoles that are unable to fully polarize with respect to the oscillating polarity of the applied field [23].

The ε′ and ε″ of the raw AT show apparent variation from 50 MHz to 13 GHz. It is because complete orientations of molecules are conducted on exposure to the equilibrium static field at low frequencies [22]. However, the ε′ and ε″ of the raw AT show unnoticeable variationfrom13 GHz to 20 GHz. It might be due to the delay in the orientations of molecules. These molecules are not able to sustain equilibrium with static fields at high frequencies[28].

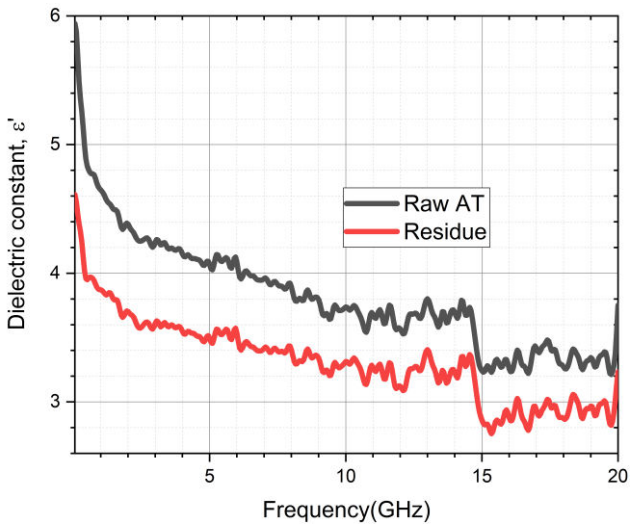

Figure-4. Dielectric constant, ε with frequency (GHz).

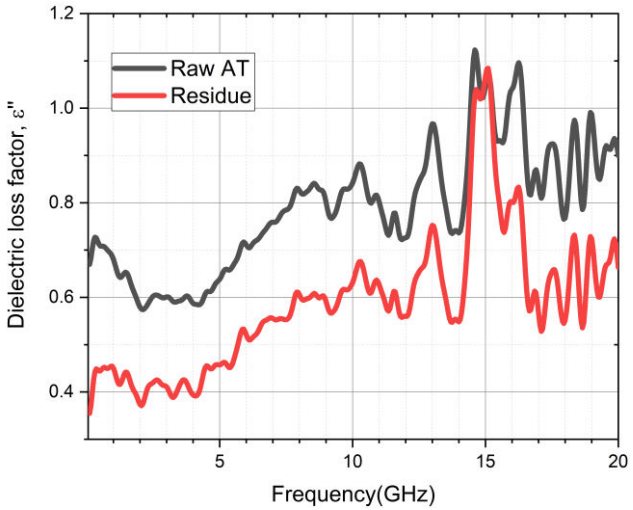

Figure-5. Dielectric loss factor, ε″ with frequency (GHz).

Figure-6 shows the variation of electrical conductivity over frequency (Hz), from 50 MHz to 20 GHz at room temperature. The electrical conductivity of both AT pellets increases gradually when frequency increases. This is due to the law of hopping conduction [27]. Low frequency shows the applied electric field forced the charge carriers to drift over large distances. However, the mean displacement of the charge carriers was reduced as the frequency increased which allows for high electrical conductivity. Moreover, the electrical conductivity of residue as shown in Figure-6 is lower than that of raw AT pellets. It could be due to the lower element content found in residue compared to raw AT pellets [24]. This is due to the extraction efficiency of elements during decoctions [25]. During decoction, the element composition of the raw AT is dispersed into the extract. Therefore, the residue AT pellet has lower conductivity than raw AT pellets.

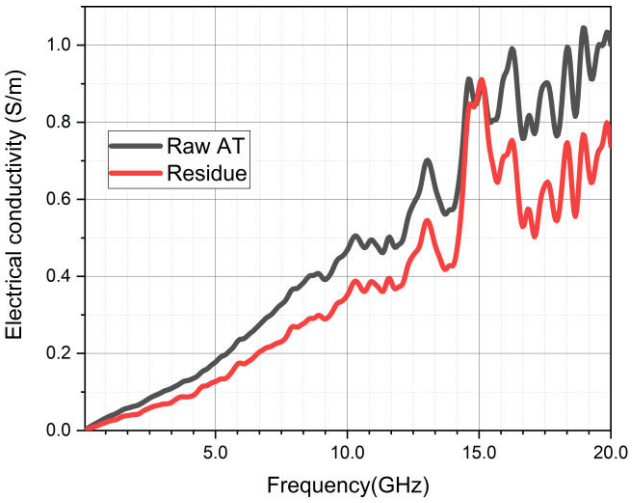

Figure-6. Electrical conductivity (S/m) with frequency (GHz).

CONCLUSIONS

The dielectric properties in terms of ε′, ε″ and σ of raw AT and residue were investigated. The frequency range from 12.5 kHz to 5 MHz and 50 MHz to 20GHz is measured using the Hioki IM3570 impedance analyser and Agilent E5071C ENA series vector network analyser respectively. The ε′ and ε″ of the raw AT pellets are higher than the residue at a constant temperature of 25 °C. The dielectric properties of residue are lower than the raw AT. Hence, an in-depth analysis study on the dielectric properties correlated with the effect of the physicochemical properties of the AT might facilitate the development of the non-destructive microwave evaluation test that deals with the quality control of medicine.

ACKNOWLEDGEMENT

The authors gratefully acknowledge the support from University Malaysia Perlis for providing facilities for this research work.

REFERENCES

[1] W. Ma *et al*. 2020. Comparison of the active components of Aster tataricus from different regions and related processed products by ultra-high performance liquid chromatography with tandem mass spectrometry', J. Sep. Sci. 43(5): 865-876.

[2] X. D. Su, H.-J. Jang, H. X. Li, Y. H. Kim, and S. Y. Yang. 2019. Identification of potential inflammatory inhibitors from Aster tataricus. Bioorg. Chem. 92: 103208.

[3] S. Wang *et al*. 2021. Comparison of the chemical profile differences of Aster tataricus between raw and processed products by metabolomics coupled with chemometrics methods. J. Sep. Sci. 44(20): 3883-3897.

[4] Y. Chen *et al*. 2019. Network pharmacology-based investigation of protective mechanism of Aster tataricus on lipopolysaccharide-induced acute lung injury. Int. J. Mol. Sci. 20(3): 543.

[5] T. Schafhauser *et al*. 2019. Antitumor astins originate from the fungal endophyte Cyanodermella asteris living within the medicinal plant Aster tataricus. Proc. Natl. Acad. Sci. U. S. A. 116(52): 26909-26917.

[6] X. Shen *et al*. 2018. Complete chloroplast genome sequence and phylogenetic analysis of Aster tataricus. Molecules. 23(10): 2426.

[7] B. Tıraş, S. Dede and F. Altay. 2019. Dielectric properties of foods. Turkish J. Agric. - Food Sci. Technol. 7(11): 1805.

[8] M. I. Hussein, D. Jithin, I. J. Rajmohan, A. Sham, E. E. M. A. Saeed and S. F. Abuqamar. 2019. Microwave characterization of hydrophilic and hydrophobic plant pathogenic fungi using open-ended coaxial probe. IEEE Access. 7: 45841-45849.

[9] A. Y. Khaled, S. A. Aziz, S. K. Bejo, N. M. Nawi, and I. A. Seman. 2018. Spectral features selection and classification of oil palm leaves infected by Basal stem rot (BSR) disease using dielectric spectroscopy. Comput. Electron. Agric. 144: 297-309.

[10] H. Yang, S. Zhang, H. Yang, Y. Yuan and E. Li. 2019. Structure stability, bond characteristics and microwave dielectric properties of co-substituted NdNbO4 ceramics. Ceram. Int. 45(3): 3620-3626.

[11] S. Ozturk, F. Kong, R. K. Singh, J. D. Kuzy, C. Li and S. Trabelsi. 2018. Dielectric properties, heating rate, and heating uniformity of various seasoning spices and their mixtures with radio frequency heating. J. Food Eng. 228: 128-141.

[12] A. Tabbagh *et al*. 2021. The case for considering polarization in the interpretation of electrical and electromagnetic measurements in the 3 kHz to 3 MHz frequency range. Surv. Geophys. 42(2): 377-397.

[13] S. Bonardd, V. Moreno-Serna, G. Kortaberria, D. D. Díaz, A. Leiva and C. Saldías. 2019. Dipolar glass polymers containing polarizable groups as dielectric materials for energy storage applications. A minireview. Polymers (Basel). 11(2): 1-10.

[14] C. H. Li, C. H. Hsieh, C. C. Hung and C. W. Cheng. 2021. Nondestructive detection of the gel state of preserved eggs based on dielectric impedance. Foods. 10(2): 1-13.

[15] A. Abdul Jaleel, A. Basheer Mohammed, P. N. P and Y. Shaikh. 2018. High quality dielectric properties of four medicinal herbs at different frequencies. Int. J. Res. Anal. Rev. 5(4): 637-641.

[16] P. Ibba, A. Falco, B. D. Abera, G. Cantarella, L. Petti, and P. Lugli. 2020. Bio-impedance and circuit parameters: An analysis for tracking fruit ripening. Postharvest Biol. Technol. 159: 110978.

[17] X. Zhou and S. Wang. 2019. Recent developments in radio frequency drying of food and agricultural products: A review. Dry. Technol. 37(3): 271-286.

[18] T. Polak, A. Polak, N. Ulrih Poklar, and N. Šegatin. 2020. Electrical admittance and dielectric properties of whipping cream. J. Food Eng. 278: 2-5.

[19] D. Grujić, B. Škipina, D. Cerović, L. Topalić-Trivunović, and A. Savić. 2021. Antibacterial and dielectric properties of textile materials modified with herbal extract of Picea omorika and the copper ferrite nanoparticles. Contemp. Mater. 12(1): 80-90.

[20] Y. Wang *et al*. 2018. Extraction and verification of miRNA from ginseng decoction. Chinese Herb. Med. 10(3): 318-322.

[21] C. Y. Beh *et al*. 2022. Dielectric and biodegradation properties of biodegradable nano-hydroxyapatite/starch bone scaffold. J. Mater. Res. Technol. 18: 3215-3226.

[22] C. Y. Beh et al. 2021. Low frequency dielectric and optical behavior on physicochemical properties of hydroxyapatite/cornstarch composite. J. Colloid Interface Sci. 600: 187-198.

[23] C. Y. Beh *et al*. 2022. Dielectric properties of hydrothermally modified potato, corn, and rice starch. Agriculture. 12(6): 783.

[24] S. F. Vaughn, J. A. Kenar, A. R. Thompson and S. C. Peterson. 2013. Comparison of biochars derived from wood pellets and pelletized wheat straw as replacements for peat in potting substrates. Ind. Crops Prod. 51: 437-443.

[25] P. Pohl *et al*. 2018. Understanding element composition of medicinal plants used in herbalism-A case study by analytical atomic spectrometry. J. Pharm. Biomed. Anal. 159: 262-271.

[26] A. S. Ravipati *et al*. 2012. Antioxidant and anti-inflammatory activities of selected Chinese medicinal plants and their relation with antioxidant content. BMC Complement. Altern. Med. 12: 5-10.

[27] M. Chaari and A. Matoussi. 2012. Electrical conduction and dielectric studies of ZnO pellets. Phys. B Condens. Matter. 407(17): 3441-3447.

[28] O. A. Bin-Dahman, M. Rahaman, D. Khastgir and M. A. Al-Harthi. 2018. Electrical and dielectric properties of poly (vinyl alcohol)/starch/graphene nanocomposites. Can. J. Chem. Eng. 96(4): 903-911.